Journal Pre-proof

Investigating phototoxicity of optical coherence tomography (OCT) imaging in porcine and human sperm

Marie Claire Aquilina , Julien Camard , Wisdom Igiogbe , Taylor Sanderson , Lucy Abbott , Darren K. Griffin , Adrian Podoleanu , Peter Ellis , Giuseppe Silvestri , Manuel J. Marques

PII: S1472-6483(25)00382-7
DOI: https://doi.org/10.1016/j.rbmo.2025.105175
Reference: RBMO 105175

To appear in: *Reproductive BioMedicine Online*

Received date: 14 March 2025
Revised date: 14 July 2025
Accepted date: 20 July 2025

Please cite this article as: Marie Claire Aquilina , Julien Camard , Wisdom Igiogbe , Taylor Sanderson , Lucy Abbott , Darren K. Griffin , Adrian Podoleanu , Peter Ellis , Giuseppe Silvestri , Manuel J. Marques , Investigating phototoxicity of optical coherence tomography (OCT) imaging in porcine and human sperm, *Reproductive BioMedicine Online* (2025), doi: https://doi.org/10.1016/j.rbmo.2025.105175

Investigating phototoxicity of optical coherence tomography (OCT) imaging in porcine and human sperm

Marie Claire Aquilina[1, *], Julien Camard[2, *,§], Wisdom Igiogbe [1], Taylor Sanderson[2], Lucy Abbott[2], Darren K. Griffin[1, 3], Adrian Podoleanu [2], Peter Ellis[1], Giuseppe Silvestri [1, 4], Manuel J. Marques[2]

[1] School of Natural Sciences, University of Kent, Canterbury, United Kingdom

[2] School of Engineering, Mathematics and Physics, University of Kent, Canterbury, United Kingdom

[3] UCL EGA Institute for Women's Health, Preimplantation Genetics Group, 86-96 Chenies Mews, London, United Kingdom[4] Conceivable Life Sciences, 160 Mercer street, New York (NY), USA

*These two authors contributed equally to this work.

[§]Corresponding author. E-mail address julien.camard@lilo.org (Julien Camard)

Abstract

Research question

Does exposure to near-infrared OCT laser radiation induce phototoxic effects in porcine and human sperm?

Design

Computer-assisted sperm analysis (CASA) was used to determine whether OCT laser illumination at or above levels typically used for imaging alters sperm motility. Flow cytometry was used to determine the impact of irradiation on sperm acrosome reaction status, DNA fragmentation, and membrane integrity. Additionally, *in vitro* time-lapse OCT imaging of a porcine cumulus-oocyte complex with irradiated sperm was performed to determine whether irradiated sperm interacts with and penetrates the cumulus oophorus. Finally, human sperm was irradiated and analysed using CASA and flow cytometric techniques.

Results

All irradiated samples showed no statistically significant difference in sperm DNA damage or CASA sperm motility parameters including average path velocity (VAP), straight line velocity (VSL) or curvilinear velocity (VCL) when compared to their matched manipulation control, suggesting that sample irradiation did not compromise spermatozoa viability even when using an optical power of more than one order of magnitude greater than that typically required to image embryos. Proof of concept OCT imaging suggested that the motility of the irradiated sperm during cumulus interaction was not affected by radiation.

Conclusions

There was no observed significant effect on boar and human sperm kinetics following near-infrared OCT laser radiation. Future work will be aimed at looking at the fertilisation process and embryo development following near-infrared OCT laser radiation.

Key words: Infrared; OCT; Optical Coherence Tomography; Phototoxicity; sperm DNA damage

Introduction

In reproductive medicine, time-lapse imaging systems (TLS) have provided new insights into the morphological processes of fertilisation and embryo development (Castellò et al., 2016; Kovacs, 2014), their clinical safety is widely accepted (Kirkegaard et al., 2012; Nakahara et al., 2010), and algorithms have been developed to identify the ideal morphokinetic parameters for achieving successful pregnancy outcomes (Chamayou et al., 2013; Cruz et al., 2012; Dal Canto et al., 2012; Petersen et al., 2016; Storr et al., 2018). However, current TLS do not offer intrinsic depth discrimination capability, making it complicated to resolve structures located at different depths. Optical Coherence Tomography (OCT) is an imaging technique that utilizes low-coherence interferometry to non-invasively produce 3D cross-sectional images of live cells and tissues of interest, both *in vitro* and *in vivo* (Huang et al., 1991; Popescu et al., 2011; Alam & Poddar, 2022; Cernat et al., 2012; Holmes, 2009; Sepehr et al., 2008). The 3D nature of OCT imaging therefore offers a novel perspective for time-lapse monitoring of early embryonic progression, providing a non-invasive method of visualizing morphokinetic events during development.

Moreover, OCT is not limited to “snapshot” imaging of cell positioning. OCT images can also be processed to understand cellular and subcellular movements by processing time-resolved images acquired at the same spatial position in the sample and interrogating the variability of the signal over time – high variability corresponds to an increasing motion of cellular and subcellular structures (Apelian et al., 2016; Ren et al., 2024). Since these motions are greatly reduced in dead cells, OCT imaging at regular time intervals therefore allows for the measurement of cellular motility and vitality while providing additional contrast on tissue morphology (Apelian et al., 2016; Kohlfaerber et al., 2022). In a reproductive context, while sperm cells are too small to be resolved directly by OCT, during fertilisation they interact with larger cells which are detectable by OCT. Thus, it may be possible to use OCT to study not only post-fertilisation embryonic development, but also the fertilisation process itself. In particular, the ability to observe changes occurring within the cumulus complex potentially offers new monitoring tools to help understand and diagnose fertility problems in couples presenting for assisted reproduction.

However, while progress has been made in the use of OCT to visualise embryonic structures at the blastocyst stage (Masuda et al., 2023) and throughout embryonic development (Karnowski et al., 2017), as yet no study has addressed its safety for gamete health, or the ability to detect peri-fertilisation events such as sperm interactions with cumulus cells. Safe exposure of oocytes and pre-implantation embryos to light exposure is discussed in a few papers (Ottosen et al., 2007; Khodavirdilou et al., 2021), though they focus on visible light exposure in the context of conventional microscopy. Safe exposure of oocytes and embryos to scanned near-infrared light in OCT is claimed in two other reports (Karnowski et al., 2017; Fluks et al., 2022;) but those claims are only supported by the observation of

the first cellular division at cleavage stage. In addition, a study by Takae *et al.* analysed the safety of OCT examination on mouse ovarian tissue and demonstrated that OCT had no effect on reproductive outcomes, including fertilisation rate and blastocyst rate, nor was it associated with increased birth defect rates (Takae et al., 2017).

No such report was found on the effect of OCT light exposure on sperm. This understanding is important since spermatozoa are particularly prone to DNA damage due to their limited DNA repair ability after spermiogenesis (García-Rodríguez et al., 2018). Although low levels of unrepaired sperm DNA damage can be repaired in the zygote following fertilisation (Ménézo et al., 2010), if sperm DNA damage exceeds the oocyte's repairing ability, there is an increased risk of implantation failure, miscarriage, abnormal foetal development, and birth defects in offspring (González-Marín et al., 2012; Vasilyeva et al., 2020; Wyck et al., 2018). Moreover, spermatozoa, when *in vivo*, are thermotactic (Bahat & Eisenbach, 2010; Rodríguez-Gil, 2019), and thus not only their genomic integrity but also their behaviour and motility patterns could potentially be affected by infrared illumination.

There is thus a critical need to establish certain key factors before OCT can be used as a tool to study fertilisation: firstly, whether OCT illumination alters sperm motility, viability or DNA fragmentation, secondly, whether sperm subjected to OCT illumination remain competent to interact with and penetrate the cumulus oophorus, and thirdly whether this cumulus interaction is itself visualisable by OCT methods. Our study therefore analysed boar and human sperm parameters following exposure to varying irradiation conditions, with the aim of providing an understanding of the genotoxic impact of broadband infrared light on spermatozoa, and also visualising the motility effects of sperm interactions with the cumulus during fertilisation. Porcine sperm were selected as a translational model of human sperm, while providing an ethically favourable and cost-effective approach for initial screening. Human sperm were subsequently evaluated to confirm the potential for clinical relevance and ensure the findings translate directly to the target species for assisted reproductive applications.

Key words: optical coherence tomography, OCT, infrared, sperm DNA damage, phototoxicity

Methods

Semen analysis

Boar semen samples were received in extender from JSR Genetics Ltd. (Southburn, United Kingdom). The iSperm automated semen analysis device (Aidmics Biotechnology Co., LTD, Taiwan) was used for sperm kinetic evaluation following irradiation. Boar sperm concentration and motility (progressive, non-progressive, and non-motile) were assessed according to the WHO 2010 criteria via the manual method (WHO, 2010). Human semen samples were collected by masturbation on the day of testing and placed in an incubator at 37°C to allow for liquefaction. Human sperm concentration, motility, and vitality were evaluated according to the WHO 2010 criteria via the manual method (WHO, 2010). Sperm motility was assessed by placing 2 x 10 µl drops of semen on opposite sides of a microscope slide and covered using 22 mm by 22 mm coverslips. Sperm motility was assessed using a x40 phase objective (x400 total magnification) and the percentages of progressive motility, nonprogressive motility and immotility were recorded. 200 sperm cells were counted in each semen drop, and the average of the replicate results was compared to the acceptable differences criteria. If the criteria were

not met, another 200 sperm cells were counted using a freshly prepared slide and a third count was performed. Vitality was assessed using 0.5% Eosin Y in 0.9% Sodium chloride (Gurr, 34197). 5 µl of semen were mixed with 5 µl of the dye on a slide. A 22 mm by 22 mm coverslip was appropriately placed and examined under a brightfield microscope. Colourless cells were counted as viable while pink stained cells were counted as non-viable. 200 sperm cells were counted. Another slide for vitality was done to count another 200 sperm cells and the average was taken to be compared to the acceptable differences criteria indicated in WHO laboratory manual for the examination and processing of human semen, 2010. If the criteria were not met, another 200 sperm cells were counted using a freshly prepared slide and a third count performed.

The LensHooke® X1 PRO (Bonraybio, Taichung, Taiwan) automated semen analysis system was used for further evaluation of sperm kinetics following irradiation. This analysis covers widely-used measures of sperm motility including average path velocity (VAP), straight line velocity (VSL) and curvilinear velocity (VCL) (Mortimer, 2000). This study was approved by the Central Research Ethics Advisory Group at the University of Kent (CREAG078-06-22) and adhered to the current legislation on research involving human subjects in the United Kingdom.

Flow Cytometry Analysis

The sperm chromatin structure assay (SCSA) was used for measuring the sperm DNA fragmentation index (%DFI). Flow cytometry analysis was performed using the BD Accuri C6 Plus flow cytometer equipped with a 488 nm, 50 mW solid-state laser (BD Biosciences, Wokingham, Berkshire, United Kingdom). The BD Accuri software (v. 1.34.1) was used for data analysis and plot generation. The SCSA protocol was followed as described elsewhere (Evenson, 2013). Briefly, semen samples were diluted to 1-2 x 10^6 sperm/mL using TNE buffer. The samples were then treated with an acid detergent solution for 30 seconds, followed by staining with an acridine orange solution to allow for the measurement of intact and fragmented DNA. Acridine orange exhibits differential binding to double-stranded and single-stranded DNA, resulting in a metachromatic shift from green to red fluorescence. A total of 15,000 sperm events per sample (5,000 sperm cells per triplicate) were analysed using the flow cytometer.

Sperm vitality and acrosome reactivity were evaluated using a staining solution composed of 1 µg/mL PNA-FITC and 1.5 µM PI in phosphate-buffered saline (Robles & Martínez-Pastor, 2013). The sperm sample was diluted in the staining solution to achieve a concentration of 1-2 x 10^6 sperm cells/mL and then analysed using the BD Accuri C6 Plus flow cytometer.

Optical system for semen irradiation and OCT imaging

The optical system used for semen irradiation and OCT imaging is presented in **Figure 1**. The system can be used in two modes as indicated by labels and coloured backgrounds. First, the 'Irradiation mode' (shown on a blue background) aimed to mimic the operation of a point-scanning OCT system, without performing imaging. Light from a continuous wave optical source (MOPA-SLD, Superlum) emitting at a wavelength of 1078 nm with a 20 nm bandwidth was coupled into an optical fibre, which was inserted into the imaging probe (IP). Inside the IP, the beam was coupled in air and scanned onto the sample using two scanning mirrors (SMX and SMY, 6215H, Novanta). The scanned light travelled through an imaging lens and a wedged glass window, reaching the sample dish placed outside the IP on top of the window. Second, the 'OCT mode' (shown on a yellow background) allowed for OCT imaging, employing a 200 kHz tuneable source (AXP50125-3 , Axsun, Excelitas Technologies) coupled to a fibre coupler,

which split light between the IP and a reference arm (fibre array, not shown). Interference spectra were detected by a balanced photodetector (PDB471C, Thorlabs).

Boar semen irradiation protocols

The irradiation protocols for the boar semen used the 'Irradiation mode' configuration. The semen sample was prepared in a standard Petri dish, shown in **Figure 2.a**. The irradiation followed three scanning protocols, A, B and C, which are described below and illustrated in **Figure 2.b**. The optical power measured at the sample was 33 ± 3 mW at 1078 nm, which is 10 to 30 times more than the power value typically used for OCT imaging (Aumann, 2019).

Protocols A and B simulated the conventional raster scanning pattern of an OCT system. Let X and Y be the axis of the horizontal plane, orthogonal to the optical axis, SMX scanned the beam rapidly along X, creating a line, and SMY scanned such line slowly along Y, altogether covering a square field of view (FOV). In Protocol A (**Figure 2.b**), the volumetric scanning frequency (f_V) was kept constant to 1.1 Hz, corresponding to a sampling density of 300 x 300 lateral points at 200 kHz, and the overall irradiation time (T_{total}) was varied from 20 to 60 seconds. In Protocol B (**Figure 2.b**), T_{total} was kept constant at 60 seconds and the scanning frequency was varied from 0.13 Hz to 1.1 Hz. A third protocol, Protocol C (**Figure 2.b**), simulated a different OCT scanning pattern, termed OCT angiography (OCT-A). In OCT-A, SMX scanned the same line a given number of times N before SMY was moved to a neighbouring Y position.

Human semen irradiation protocol

Human semen samples were irradiated following Protocol D (**Figure 2.b**). In Protocol D, both the scanning frequency and irradiation time were fixed (f_V = 1.1 Hz, T_{total} = 60 seconds) and the irradiation power was varied. The semen samples were separated into three groups: low-power, high-power, and a non-irradiated control group. The low and high-power conditions corresponded to an incident optical power on the sample of 4.9 ± 0.3 mW and 33 ± 3.0 mW, respectively, at a wavelength of 1078 nm. The power values were measured using a commercial power-meter (PM100D, Thorlabs).

Statistical analysis for sperm parameters

Statistical analysis, performed using the SPSS 28.0 software (SPSS Inc., Chicago, IL, USA), was performed to evaluate whether irradiated samples (at different imaging protocols) showed significant differences with their matched manipulation control. The Kolmogorov-Smirnov test was used to assess normality and groups were compared using the Kruskal-Wallis test. The number of degrees of freedom, the H value and p value are given in tables for all comparisons. For all statistical comparisons, significance was considered as p-value < 0.05.

OCT imaging protocol for sperm incubation with cumulated oocytes

For OCT imaging of cumulus-oocyte complexes with added irradiated sperm, porcine COCs were retrieved from abattoir material as described in previous publications (Silvestri et al., 2020; Serrano

Albal et al., 2022). This procedure yields mature oocytes surrounded by cumulus cells, but whose fertilisation potential is highly dependent on the quality of the ovaries received from the abattoir. For the purposes of this study they therefore serve as an indicator of sperm interaction with cumulus cells only, not as a true readout of fertilisation ability. Matured COCs were pipetted into a multi-well Petri dish (Primo Vision), as shown in **Figure 3.a**. The 'OCT mode' setup (see **Figure 1**) was used to track the porcine COCs inside the incubator. Two wells each containing a single COC were imaged (n=2), one with added irradiated boar sperm (ID), and a control dish with no sperm (CD). The incident optical power with static beam was 1.3 mW at 1078 nm. OCT volumes of dish ID were acquired every 5 minutes for 4 hours, and OCT volumes of dish CD were acquired every 5 minutes for 3 hours.

The OCT stacks were processed with an in-house LabVIEW software generating OCT images from raw OCT data and with an in-house Fiji (ImageJ) macro performing the steps of image stacking, image straightening, slicing and construction of depth-specific time series, masking and contrast enhancement (see **Figure 3.b**). For each dataset, and for the processing steps presented hereafter, slicing was performed at two separate depths, one intersecting the oocyte and part of the cumulus cells around the oocyte ('through' slice), another above the oocyte, only intersecting the cumulus cells ('away' slice).

Co-localisation analysis

Co-localisation methods aim to evaluate the correlation between the pixel-wise intensity of two images. Here, a co-localisation analysis was used to quantitatively assess sample movement in the cumulus cells area, for both a control COC and a COC mixed with the irradiated sperm sample. Co-localization analysis was performed using the JACoP plugin (Bolte and Cordelières, 2006). The Manders coefficient represents the fraction of the total intensity in the current image that co-localises with the intensities in a reference image. The evolution of Manders coefficient M2 for each image between timepoints t_1 and t_N was evaluated, where the first image at timepoint t_0 served as the reference image.

Logarithm Intensity Variance

The co-localisation analysis was complemented with the visualisation of the Logarithm Intensity Variance (LIV). The LIV calculation measures the magnitude of the signal fluctuation on the total duration of the timelapse, highlighting movements in the sample (El Sadek et al., 2020). LIV processing was performed across 35 timepoints, acquired during a total time of 2 hours and 50 minutes, for both the control COC and the COC mixed with the irradiated sperm sample. The algorithm used to build a LIV mapping of the sample is adapted from a Python software developed by El-Sadek *et al.* (El Sadek et al., 2020).

Results

In initial experiments, we focused on determining how different OCT scanning protocols affect sperm function in relation to vitality, motility and acrosome status. Specifically, protocols were designed to study: (1) the impact of varying the total amount of energy received by the sample, while keeping the irradiation frequency constant (Protocol A), (2) the impact of varying the irradiation frequency - i.e. the time between two successive exposures of spermatozoa - at a constant dose level (Protocol B); and (3) whether transient exposure to higher frequency irradiation for part of the scan had a deleterious effect (Protocol C).

Boar sperm parameters are not altered by increasing irradiation time at constant scanning frequency and power (Protocol A)

Exposure of boar spermatozoa (n = 3 ejaculates tested) in a commercial extender to varying overall exposure times (20 to 60 seconds) resulted in no significant change in the tested sperm parameters (progressive motility, total motility, vitality, acrosome reactivity and sperm DNA damage, see **Table 1**).

With regards to sperm kinetic (**Figure 4.A**) parameters, the control showed a similar VAP, VSL and VCL for the different irradiation times (20 seconds, 40 seconds and 60 seconds).

TABLE 1 HERE

Boar sperm parameters are not altered by increasing scanning frequency at constant irradiation time and power (protocol B)

Exposure of boar spermatozoa (n = 5 ejaculates tested) in a commercial extender to varying scanning frequency, at an irradiation time of 60 seconds, resulted in no significant change in the tested sperm parameters (progressive motility, total motility, vitality, acrosome reactivity and sperm DNA damage, see **Table 2**).

With regards to sperm kinetic (**Figure 4.B**) parameters, the control showed a similar VAP, VSL and VCL for the varying scanning frequencies.

TABLE 2 HERE

Boar sperm parameters are not altered by OCT-A line scan repetition rate at constant irradiation time, scanning frequency and power (Protocol C)

Exposure of boar spermatozoa (n = 3 ejaculates tested) in a commercial extender to various numbers of OCT-A line scan repetitions (5 N, 10 N and 20 N) resulted in no significant change in the tested sperm parameters (progressive motility, total motility, vitality, acrosome reactivity and sperm DNA damage, see **Table 3)**.
With regards to sperm kinetic (**Figure 4.C**) parameters, the control showed a similar VAP, VSL and VCL for the varying number of OCT-A line scan repetitions.

TABLE 3 HERE

Boar sperm remain competent to interact with and enter the cumulus following OCT irradiation

Having demonstrated that none of the above exposure parameters altered sperm motility, acrosome status or DNA fragmentation even at values higher than those typically used for OCT imaging, we conducted a pilot study to test sperm behaviour in co-culture with cumulus-oocyte complexes (COCs), to determine whether this interaction was perturbated by OCT imaging. The 'OCT mode' setup was employed to monitor the *in situ* interaction of sperm with COCs (n = 2 COCs tested) within the incubator environment (see **Supplementary Video**). The first COC was co-incubated with irradiated boar spermatozoa (dish ID), while the second COC (dish CD), served as a control, i.e. without the addition of sperm. The objective of this experiment was to compare the dynamics in the OCT image series between both samples, and especially to determine whether we could detect the cellular motions provoked by sperm interaction with and penetration of the cumulus cell mass.

From the OCT time series, two depths were tracked in time for each of ID and CD. Those depths were chosen to include a portion of the cumulus cells, one intercepting the oocyte and masked as shown in **Figure 3.b**, and one below the oocyte. **Figure 5.a** shows the result of the co-localisation analysis (M2 coefficient) for both depths in each of ID and CD. For CD, The M2 value is high for the first frames, and slowly decreases throughout the time series for CD while staying above 0.7, indicating very small frame to frame variation i.e. slow dynamics. For ID, plotting of the M2 value showed a linear decrease between frames 1 to 6 (30 min duration), and a second linear decrease with a lower slope for the rest of the time series, down to M2 values between 0.3 and 0.4. These results highlight an additional dynamic activity in ID as compared to CD, probably resulting from sperm movement within the cumulus cells, and suggesting a fair level of sperm mobility.

To validate the co-localisation analysis, LIV maps of ID and CD at the same depths of interest were computed and are presented in 5.b to 5.e. LIV maps 5.d and 5.e, corresponding to ID, showed more green areas in the cumulus cells when compared with maps 5.b and 5.c, corresponding to CD. This indicates a much higher dynamic activity in ID, further validating the conclusions drawn from the co-localisation analysis. Of note, the high LIV signal in 5.d and 5.e is present throughout the cumulus mass and is not confined to the surface layer, indicating that the sperm are fully penetrating the cumulus during this experiment.

Overall, while this is a pilot study, this data indicates that OCT is capable of detecting the motions of cumulus cells as sperm burrow between them, and that spermatozoa subjected to OCT illumination retain the ability to bind to and enter deep within the cumulus.

Human sperm show no adverse effects of OCT illumination even at powers exceeding typical imaging (Protocol D)

Based on the above, boar semen show no observable difference between irradiated and non-irradiated sperm following varying irradiation conditions. However, boar sperm chromatin is typically more resistant to damage than human sperm chromatin, in particular oxidative stress and DNA fragmentation (Enciso et al., 2011). We therefore tested the effect of irradiation of human semen (n = 6 ejaculates tested from 3 donors) at different power levels using the harshest set of parameters previously tested on boar sperm (Protocol D). For this analysis, we again used laser power levels substantially exceeding those typically used for OCT imaging, to determine whether this provoked any detectable change in semen parameters.

Exposure of human semen samples at 1.10 Hz scanning frequency for 60 seconds at varied power (4.9 ± 0.3 mW and 33 ± 3 mW at 1078 nm) resulted in no significant change in the tested parameters across the different groups (see **Table 4**). With regards to sperm kinetic (**Figure 4.D**) parameters, the control showed a similar VAP, VSL and VCL for the two different irradiation powers tested.

TABLE 4 HERE

Discussion

While multiple studies have focused on the potential *in vitro* and *in vivo* use of OCT for imaging during embryogenesis, few have explored the safety of the OCT system in relation to genotoxic effects, and none have studied its effects on sperm. This study is therefore the first systematic study to investigate the potential genotoxic impact of broadband infrared radiation on boar and human sperm. We found that there is no observable effect on sperm parameters following exposure to broadband infrared irradiation, and moreover that OCT can detect the motion of cumulus cells caused by interactions with live sperm cells. Thus, OCT can in principle be used as a safe method to enable 3D morphokinetic investigation of the very earliest events in mammalian life, even prior to and during fertilisation.

In particular, we show that boar sperm exposed to broadband infrared light around 1060 nm at varying exposure times and scanning frequencies showed no alteration in vitality, motility patterns, acrosome integrity or DNA fragmentation, even when using power levels 10 to 30 times higher than commonly employed in OCT imaging. This result was replicated for human sperm, and even at the highest power level of 33 mW, there was no effect on sperm parameters, including DNA damage levels. It is also worth noting that while the boar samples used in this study had very low baseline DNA fragmentation of 2-3% (typical for stud animals highly selected for fertility), the volunteer donor human semen samples used in this study had moderate baseline DNA fragmentation index (DFI) levels of around 30%. This is

at the high end of normal DFI for unselected humans, likely reflecting the fact that our donors were not required to observe the strict rules on ejaculation frequency typically used in diagnostic semen analysis. Therefore the lack of a detectable change in DNA fragmentation in response to OCT illumination is a genuine finding and is not due to any lack of sensitivity in our DFI detection protocol.

We also observed no difference in acrosome reactivity or motility in our irradiated samples. The acrosome reaction is a critical process for successful fertilisation (Hirohashi & Yanagimachi, 2018; Tello-Mora et al., 2018). The finding that infrared illumination does not impact the proportion of boar sperm undergoing the acrosome reaction suggests that the irradiation does not compromise the structural or functional integrity of the sperm membrane, confirming the preserved fertilisation potential of spermatozoa. Interestingly, some studies have shown improved sperm motility and calcium transport, as well as no significant change in sperm DNA damage levels following low-power monochromatic visible irradiation at 633 nm (Preece et al., 2017 and Breitbart et al., 1996), and at 905 nm (Firestone et al., 2013). We however observed no difference in sperm motility following infra-red illumination likely due to the different irradiation protocols followed and different wavelength.

How then could OCT be deployed within the clinical environment? We envisage several potential areas where it may be useful. In particular, the high-resolution depth sectioning ability of OCT imaging has the potential to provide additional information for selecting the optimal embryo for elective transfer, mitigating risks linked to multi-embryo transfer such as multiple pregnancy. The incorporation of OCT technology into traditional time-lapse systems could also allow for the identification of potential embryonic defects that might not be observable through conventional analysis methods. Most pertinently to this study on gamete safety, OCT could potentially be used for guiding the positioning of microinjection needles during the intracytoplasmic sperm injection (ICSI) procedure, helping to avoid damage to the meiotic spindle. Finally, as we demonstrate here, we can observe movements of cumulus cells during co-incubation with sperm – potentially this could be used to track the progress of cumulus penetration and help diagnose patients with fertility problems affecting this process.

Limitations of the study and directions for future work

The primary limitation of this study is the low number of samples available for the pilot data on cumulus penetration (n=2 COCs) and human donor studies (n=6 from 3 donors). Thus, we do not claim that these findings are sufficient to support clinical use of OCT at this stage. Rather than extrapolating safety conclusions directly to clinical practice, our aim was to establish a foundation for assessing potential DNA or functional damage using sensitive and relevant biological readouts. These pilot data provide preliminary reassurance that the tested OCT parameters do not induce overt harm under our experimental conditions, but we fully acknowledge that broader validation is essential.

A further limitation is that acrosome integrity was only assessed in boar spermatozoa and not in human spermatozoa. This will be assessed in future studies. Finally, while our work provides encouraging preliminary data to suggest that acute OCT illumination has no adverse effects on human semen samples, a wider study including donors with varying levels of baseline sperm parameters will be needed to establish its utility in patient populations. For longer term OCT monitoring of embryo

development, further research will also need to address potential effects of cumulative / long-term OCT exposure.

While this study serves as a proof of concept to show that sperm retain the ability to penetrate the cumulus following irradiation, and that OCT can detect the movements caused by this, further experimentation will be required to understand how robust this is to the experimental setup, and how defects in different stages of fertilisation affect the motions visible by OCT. In particular, mouse models with defects in cumulus penetration (e.g. deficiencies in hyaluronidase or acrosomal proteases) (Park et al., 2019; Kawano et al., 2010) vs zona binding (reviewed by Inoue et al., 2007) vs oolemma binding (e.g. Izumo1 deficiency) (Matsumura er al., 2022) could reveal how sensitive OCT imaging is to different stages of the fertilisation process, and whether this could be useful in defining different groups of infertile patients.

In terms of observing the moment of fertilisation itself, although we obtained OCT images during cumulus penetration, we were not able to definitively observe fertilisation due to difficulties obtaining viable oocytes from abattoir material. Thus, the results from this feasibility study warrant further investigation into analysing the fertilisation and embryo development potential following gamete and embryo irradiation to develop a more comprehensive embryo imaging technology. Additional testing will involve the use of an integrated time-lapse system utilizing OCT technology to optimize embryo monitoring and selection throughout the entire early embryonic development.

Extensive testing in animal model systems will necessarily be required before contemplating work on human embryos, including demonstration of successful fertilisation and early embryo development. Given typical success rates from fertilisation through to blastocyst formation of ~80% in murine IVF (Vasudevan et al., 2010) and ~30% in porcine IVF (Chen et al. 2022), a cohort size of approximately 1100 embryos (mouse) or 1250 embryos (pig) per experimental group would be required to detect a 5-percentage point change in blastulation rates. Following this, further work should involve fertilization and embryo development endpoints in appropriate preclinical models. If safety is confirmed in these expanded studies, then potential clinical applications—such as real-time sperm selection or diagnostic imaging—could be considered. Until then, we view our findings as an initial step toward defining the experimental and safety framework required for such translation.

Acknowledgements

The research was supported by the Summer Vacation Research Competition 2022, Graduate Researcher College, University of Kent.

JC, MJM, AP and DG acknowledge the BBSRC for the research grant 5DHiResE (BB/S016643/1).

GS, PE and AP thank the MRC, Impact Accelerator Account, project 18557.

Authors acknowledge Superlum Diodes Ltd. for the loan of the MOPA source prototype.

Conflict of Interest

The authors Dr Marie Claire Aquilina and Dr Peter Ellis are involved in providing a commercial sperm DNA damage testing service at the University of Kent.

GS received consulting fees from IVF 2.0 (a company that markets sperm selection software); this was in Dec 2022. GS is currently an employee and shareholder of Conceivable Life Sciences (a company that develops ART automation equipment, including systems for sperm preparation)

Disclosures
AP and MJM, co-inventors of patents in the name of the University of Kent.

Authorship Contribution Statement (1) the conception and design of the study: GS, MJM, JC, MCA, PJE, experimental work and data acquisition: WI, TS, LA, MCA, JC, MJM, analysis and interpretation of data: MCA, JC, PJE, GS, MJM, WI, TS, LA, AP, DG (2) drafting the article or revising it critically for important intellectual content: MCA; JC; PJE; MM (3) All authors read and approved the final manuscript.

References

Alam, Z., & Poddar, R. (2022). An in-vivo depth-resolved imaging of developing zebrafish microstructure and microvasculature using swept-source optical coherence tomography angiography. *Optics and Lasers in Engineering*, *156*, 107087. https://doi.org/10.1016/j.optlaseng.2022.107087

Apelian, C., Harms, F., Thouvenin, O., & Boccara, A. C. (2016). Dynamic full field optical coherence tomography: subcellular metabolic contrast revealed in tissues by interferometric signals temporal analysis. Biomedical optics express, 7(4), 1511-1524.

Aumann, S., Donner, S., Fischer, J., & Müller, F. (2019). Optical Coherence Tomography (OCT): Principle and Technical Realization. In J. F. Bille (Ed.), *High Resolution Imaging in Microscopy and Ophthalmology: New Frontiers in Biomedical Optics* (pp. 59–85). Springer International Publishing. https://doi.org/10.1007/978-3-030-16638-0_3

Bahat, A., & Eisenbach, M. (2010). Human sperm thermotaxis is mediated by phospholipase C and inositol trisphosphate receptor Ca2+ channel. Biology of reproduction, 82(3), 606–616. https://doi.org/10.1095/biolreprod.109.080127

Castellò, D., Motato, Y., Basile, N., Remohí, J., Espejo-Catena, M., & Meseguer, M. (2016). How much have we learned from time-lapse in clinical IVF? *MHR: Basic Science of Reproductive Medici*, *22*. https://doi.org/10.1093/molehr/gaw056

Cernat, R., Tatla, T. S., Pang, J., Tadrous, P. J., Bradu, A., Dobre, G., Gelikonov, G., Gelikonov, V., & Podoleanu, A. Gh. (2012). Dual instrument for in vivo and ex vivo OCT imaging in an ENT department. *Biomedical Optics Express*, *3*(12), 3346–3356. https://doi.org/10.1364/BOE.3.003346

Chamayou, S., Patrizio, P., Storaci, G., Tomaselli, V., Alecci, C., Ragolia, C., Crescenzo, C., & Guglielmino, A. (2013). The use of morphokinetic parameters to select all embryos with full capacity to implant. *Journal of Assisted Reproduction and Genetics*, *30*(5), 703–710. https://doi.org/10.1007/s10815-013-9992-2

Chen, P.R., Uh, K., Redel, B.K., Reese, E.D., Prather, R.S. & Lee, K. (2022). Production of Pigs From Porcine Embryos Generated in vitro. *Front. Anim. Sci. 3:826324*. https://doi.org/10.3389/fanim.2022.826324

Cruz, M., Garrido, N., Herrero, J., Pérez-Cano, I., Muñoz, M., & Meseguer, M. (2012). Timing of cell division in human cleavage-stage embryos is linked with blastocyst formation and quality. *Reproductive Biomedicine Online*, *25*(4), 371–381. https://doi.org/10.1016/j.rbmo.2012.06.017

Dal Canto, M., Coticchio, G., Mignini Renzini, M., De Ponti, E., Novara, P. V., Brambillasca, F., Comi, R., & Fadini, R. (2012). Cleavage kinetics analysis of human embryos predicts development to blastocyst and implantation. *Reproductive BioMedicine Online*, *25*(5), 474–480. https://doi.org/10.1016/j.rbmo.2012.07.016

Enciso, M., Johnston, S. D., & Gosálvez, J. (2011). Differential resistance of mammalian sperm chromatin to oxidative stress as assessed by a two-tailed comet assay. Reproduction, fertility, and development, 23(5), 633–637. https://doi.org/10.1071/RD10269

Evenson, D. P. (2013). Sperm Chromatin Structure Assay (SCSA®). In D. T. Carrell & K. I. Aston (Eds.), *Spermatogenesis: Methods and Protocols* (pp. 147–164). Humana Press. https://doi.org/10.1007/978-1-62703-038-0_14

Firestone, R. S., Esfandiari, N., Moskovtsev, S. I., Burstein, E., Videna, G. T., Librach, C., Bentov, Y., & Casper, R. F. (2013). The effects of low-level laser light exposure on sperm motion characteristics and DNA damage. Journal of andrology, 33(3), 469–473. https://doi.org/10.2164/jandrol.111.013458

Fluks, M., Tamborski, S., Szkulmowski, M., & Ajduk, A. (2022). Optical coherence microscopy allows for quality assessment of immature mouse oocytes. Reproduction (Cambridge, England), 164(3), 83–95. https://doi.org/10.1530/REP-22-0178

García-Rodríguez, A., Gosálvez, J., Agarwal, A., Roy, R., & Johnston, S. (2018). DNA Damage and Repair in Human Reproductive Cells. *International Journal of Molecular Sciences*, *20*(1), 31. https://doi.org/10.3390/ijms20010031

González-Marín, C., Gosálvez, J., & Roy, R. (2012). Types, Causes, Detection and Repair of DNA Fragmentation in Animal and Human Sperm Cells. *International Journal of Molecular Sciences*, *13*(11), 14026–14052. https://doi.org/10.3390/ijms131114026

Holmes, J. (2009). In vivo real-time optical coherence tomography imaging of Drosophila for cardiovascular research. *Nature Methods*, *6*(10), Article 10. https://doi.org/10.1038/nmeth.f.270

Huang, D., Swanson, E. A., Lin, C. P., Schuman, J. S., Stinson, W. G., Chang, W., Hee, M. R., Flotte, T., Gregory, K., & Puliafito, C. A. (1991). Optical coherence tomography. Science (New York, N.Y.), 254(5035), 1178–1181. https://doi.org/10.1126/science.1957169

Inoue, N., Yamaguchi, R., Ikawa, M., & Okabe, M. (2007). Sperm-egg interaction and gene manipulated animals. Society of Reproduction and Fertility supplement, 65, 363–371.

Karnowski, K., Ajduk, A., Wieloch, B., Tamborski, S., Krawiec, K., Wojtkowski, M., & Szkulmowski, M. (2017). Optical coherence microscopy as a novel, non-invasive method for the 4D live imaging of early mammalian embryos. Scientific reports, 7(1), 4165.

Kawano, N., Kang, W., Yamashita, M., Koga, Y., Yamazaki, T., Hata, T., Miyado, K., & Baba, T. (2010). Mice lacking two sperm serine proteases, ACR and PRSS21, are subfertile, but the mutant sperm are infertile in vitro. Biology of reproduction, 83(3), 359–369. https://doi.org/10.1095/biolreprod.109.083089

Khodavirdilou, R., Pournaghi, M., Oghbaei, H., Rastgar Rezaei, Y., Javid, F., Khodavirdilou, L., Shakibfar, F., Latifi, Z., Hakimi, P., Nouri, M., Fattahi, A., & Dittrich, R. (2021). Toxic effect of light on oocyte and pre-implantation embryo: a systematic review. Archives of toxicology, 95(10), 3161–3169. https://doi.org/10.1007/s00204-021-03139-4

Kirkegaard, K., Hindkjaer, J. J., Grøndahl, M. L., Kesmodel, U. S., & Ingerslev, H. J. (2012). A randomized clinical trial comparing embryo culture in a conventional incubator with a time-lapse incubator. *Journal of Assisted Reproduction and Genetics*, *29*(6), 565–572. https://doi.org/10.1007/s10815-012-9750-x

Kohlfaerber, T., Pieper, M., Münter, M., Holzhausen, C., Ahrens, M., Idel, C., Bruchhage, K.L., Leichtle, A., König, P., Hüttmann, G. and Schulz-Hildebrandt, H. (2022). Dynamic microscopic optical coherence tomography to visualize the morphological and functional micro-anatomy of the airways. Biomedical Optics Express, 13(6), 3211-3223.

Kovacs, P. (2014). Embryo selection: The role of time-lapse monitoring. *Reproductive Biology and Endocrinology*, *12*(1), 124. https://doi.org/10.1186/1477-7827-12-124

Leung, H. M., Wang, M. L., Osman, H., Abouei, E., MacAulay, C., Follen, M., Gardecki, J. A., & Tearney, G. J. (2020). Imaging intracellular motion with dynamic micro-optical coherence tomography. Biomed. Opt. Express, 11(5), 2768–2778. https://doi.org/10.1364/BOE.390782

Masuda, Y., Hasebe, R., Kuromi, Y., Hishinuma, M., Ohbayashi, T., & Nishimura, R. (2023). Hatchability evaluation of bovine IVF embryos using OCT-based 3d image analysis. Journal of Reproduction and Development, 69(5), 239-245.

Matsumura, T., Noda, T., Satouh, Y., Morohoshi, A., Yuri, S., Ogawa, M., Lu, Y., Isotani, A., & Ikawa, M. (2022). Sperm IZUMO1 Is Required for Binding Preceding Fusion With Oolemma in Mice and Rats. Frontiers in cell and developmental biology, 9, 810118. https://doi.org/10.3389/fcell.2021.810118

Ménézo Y, Dale B, Cohen M. DNA damage and repair in human oocytes and embryos: a review. Zygote. (2010). 18(4):357-65. doi: 10.1017/S0967199410000286. Epub 2010 Jul 21. PMID: 20663262.

Mortimer, S.T. (2000). CASA--practical aspects. *J Androl. 21*(4):515-24.

Nakahara, T., Iwase, A., Goto, M., Harata, T., Suzuki, M., Ienaga, M., Kobayashi, H., Takikawa, S., Manabe, S., Kikkawa, F., & Ando, H. (2010). Evaluation of the safety of time-lapse observations for human embryos. *Journal of Assisted Reproduction and Genetics*, *27*(2–3), 93–96. https://doi.org/10.1007/s10815-010-9385-8

Ottosen, L. D., Hindkjaer, J., & Ingerslev, J. (2007). Light exposure of the ovum and preimplantation embryo during ART procedures. Journal of assisted reproduction and genetics, 24(2-3), 99–103. https://doi.org/10.1007/s10815-006-9081-x

Park, S., Kim, Y. H., Jeong, P. S., Park, C., Lee, J. W., Kim, J. S., Wee, G., Song, B. S., Park, B. J., Kim, S. H., Sim, B. W., Kim, S. U., Triggs-Raine, B., Baba, T., Lee, S. R., & Kim, E. (2019). SPAM1/HYAL5 double deficiency in male mice leads to severe male subfertility caused by a cumulus-oocyte complex penetration defect. FASEB journal : official publication of the Federation of American Societies for Experimental Biology, 33(12), 14440–14449. https://doi.org/10.1096/fj.201900889RRR

Petersen, B. M., Boel, M., Montag, M., & Gardner, D. K. (2016). Development of a generally applicable morphokinetic algorithm capable of predicting the implantation potential of embryos transferred on Day 3. *Human Reproduction (Oxford, England)*, *31*(10), 2231–2244. https://doi.org/10.1093/humrep/dew188

Popescu, D. P., Choo-Smith, L.-P., Flueraru, C., Mao, Y., Chang, S., Disano, J., Sherif, S., & Sowa, M. G. (2011). Optical coherence tomography: Fundamental principles, instrumental designs and biomedical applications. *Biophysical Reviews*, *3*(3), 155. https://doi.org/10.1007/s12551-011-0054-7

Preece, D., Chow, K. W., Gomez-Godinez, V., Gustafson, K., Esener, S., Ravida, N., Durrant, B., & Berns, M. W. (2017). Red light improves spermatozoa motility and does not induce oxidative DNA damage. Scientific reports, 7, 46480. https://doi.org/10.1038/srep46480

Raghunathan, R., Singh, M., Dickinson, M. E., & Larin, K. V. (2016). Optical coherence tomography for embryonic imaging: A review. *Journal of Biomedical Optics*, *21*(5), 050902. https://doi.org/10.1117/1.JBO.21.5.050902

Ren, C., Hao, S., Wang, F., Matt, A., Amaral, M.M., Yang, D., Wang, L. and Zhou, C. (2024). Dynamic contrast optical coherence tomography (DyC-OCT) for label-free live cell imaging. Commun Biol 7, 278. https://doi.org/10.1038/s42003-024-05973-5

Robles, V., & Martínez-Pastor, F. (2013). Flow cytometric methods for sperm assessment. Methods in Molecular Biology (Clifton, N.J.), 927, 175–186. https://doi.org/10.1007/978-1-62703-038-0_16

Rodríguez-Gil J. E. (2019). Photostimulation and thermotaxis of sperm: Overview and practical implications in porcine reproduction. Theriogenology, 137, 8–14. https://doi.org/10.1016/j.theriogenology.2019.05.031

Serrano Albal, M., Silvestri, G., Kiazim, L. G., Vining, L. M., Zak, L. J., Walling, G. A., Haigh, A. M., Harvey, S. C., Harvey, K. E., & Griffin, D. K. (2022). Supplementation of porcine in vitro maturation medium with FGF2, LIF, and IGF1 enhances cytoplasmic maturation in prepubertal gilts oocytes and improves embryo quality. Zygote (Cambridge, England), 30(6), 801–808. https://doi.org/10.1017/S0967199422000284

Sepehr, A., Armstrong, W. B., Guo, S., Su, J., Perez, J., Chen, Z., & Wong, B. J. F. (2008). Optical coherence tomography of the larynx in the awake patient. *Otolaryngology--Head and Neck Surgery*, *138*(4), 425–429. https://doi.org/10.1016/j.otohns.2007.12.005

Silvestri, G., Rathje, C. C., Harvey, S. C., Gould, R. L., Walling, G. A., Ellis, P. J. I., Harvey, K. E., & Griffin, D. K. (2020). Identification of optimal assisted aspiration conditions of oocytes for use in porcine in vitro maturation: A re-evaluation of the relationship between the cumulus oocyte complex and oocyte quality. Veterinary Medicine and Science, 7(2), 465–473. https://doi.org/10.1002/vms3.378

Storr, A., Venetis, C., Cooke, S., Kilani, S., & Ledger, W. (2018). Time-lapse algorithms and morphological selection of day-5 embryos for transfer: A preclinical validation study. *Fertility and Sterility*, *109*(2), 276-283.e3. https://doi.org/10.1016/j.fertnstert.2017.10.036

Takae, S., Tsukada, K., Sato, Y., Okamoto, N., Kawahara, T., & Suzuki, N. (2017). Accuracy and safety verification of ovarian reserve assessment technique for ovarian tissue transplantation using optical coherence tomography in mice ovary. Scientific reports, 7, 43550. https://doi.org/10.1038/srep43550

Vasilyeva, T. A., Marakhonov, A. V., Sukhanova, N. V., Kutsev, S. I., & Zinchenko, R. A. (2020). Preferentially Paternal Origin of De Novo 11p13 Chromosome Deletions Revealed in Patients with Congenital Aniridia and WAGR Syndrome. *Genes*, *11*(7), 812. https://doi.org/10.3390/genes11070812

Vasudevan, K., Raber, J., & Sztein, J. (2010). Fertility comparison between wild type and transgenic mice by in vitro fertilization. *Transgenic Res., 19*(4):587-94. https://doi.org/10.1007/s11248-009-9336-2

World Health Organization (2010). WHO Laboratory Manual for the Examination and Processing of Human Semen. 5th Edition, Geneva.

Wyck, S., Herrera, C., Requena, C. E., Bittner, L., Hajkova, P., Bollwein, H., & Santoro, R. (2018). Oxidative stress in sperm affects the epigenetic reprogramming in early embryonic development. *Epigenetics & Chromatin*, *11*(1), 60. https://doi.org/10.1186/s13072-018-0224-y

Legends to tables

Table 1: Parameters of boar sperm following irradiation with varying overall irradiation time at constant scanning frequency (Protocol A). Values represent the average ± standard error. This experiment was repeated 3 times using 3 different boar ejaculates. Degrees of freedom: 3, given four sample groups with different exposure conditions. Control samples are non-irradiated samples.

Overall irradiation time (seconds)	Progressive motility (%)	Total motility (%)	Vitality (%)	Acrosome Intact (%)	DFI (%)
0 (Control)	31.0 ± 16.6	48.2 ± 19.8	75.8 ± 10.5	73.3 ± 10.6	2.9 ± 0.4
20	14.7 ± 3.2	42.7 ± 11.9	90.4 ± 4.8	88.5 ± 4.5	2.3 ± 0.2
40	24.7 ± 18.7	35.3 ± 16.8	89.9 ± 4.6	87.5 ± 4.5	2.6 ± 0.3
60	23.7 ± 18.0	34.8 ± 14.3	84.7 ± 7.1	82.4 ± 7.3	2.6 ± 0.3
p value	0.83	0.78	0.66	0.72	0.66
H value	0.9	1.1	1.56	1.36	1.59

Table 2: Parameters of boar sperm following irradiation with varying scanning frequency at constant overall irradiation time (Protocol B). Values represent the average ± standard error. This experiment was repeated 5 times using 5 different boar ejaculates. Degrees of freedom: 3, given four sample groups with different exposure conditions. Control samples are non-irradiated samples.

Scanning frequency (Hz)	Progressive motility (%)	Total motility (%)	Vitality (%)	Acrosome Intact (%)	DFI (%)
Control	30. 9± 3.9	64.5 ± 6.8	94.3 ± 1.8	92.6 ± 2.1	2.6 ± 0.6
1.1	24.4 ± 5.1	61.3 ± 11.2	93.3 ± 1.7	91.7 ± 2.0	2.7 ± 0.5
0.4	24.3 ± 4.6	62.8 ± 9.7	93.5 ± 1.9	92.1 ± 2.1	2.5 ± 0.4
0.13	21.5 ± 2.9	60 ± 8.5	93.4 ± 1.7	92.1 ± 2.0	2.2 ± 0.3
p value	0.6	0.97	0.91	0.96	0.92
H value	1.86	0.26	0.55	0.33	0.5

Table 3: Parameters of boar sperm following irradiation with varying OCT-A line scan repetitions (Protocol C). Values represent the average ± standard error. This experiment was repeated 3 times using 3 different boar ejaculates. Degrees of freedom: 3, given four sample groups with different exposure conditions. Control samples are non-irradiated samples.

OCT-A line scan repetitions	Progressive motility (%)	Total motility (%)	Vitality (%)	Acrosome Intact (%)	DFI (%)
Control	11.3 ± 3.9	32.2 ± 6.4	93.0 ± 2.3	90.3 ± 2.8	2.0 ± 0.2
5 N	13.3 ± 0.7	39.8 ± 0.8	90.8 ± 0.3	88.2 ± 0.7	2.0 ± 0.3

10 N	13 ± 2.6	32.7 ± 4.1	91.1 ± 3.8	89.1 ± 4.8	1.9 ± 0.3
20 N	9.3 ± 1.7	24.0 ± 5.5	91.6 ± 2.1	89.2 ± 2.7	2.1 ± 0.2
p value	0.676	0.207	0.931	0.972	0.989
H value	3.33	4.71	1.36	1.15	0.28

Table 4: Parameters of human sperm following varying irradiation power values (Protocol D). Values represent the average ± standard error. This experiment was repeated using 6 different human ejaculates from 3 donors. Degrees of freedom: 2, given three sample groups with different exposure conditions. Control samples are non-irradiated samples.

	Progressive motility (%)	**Total motility (%)**	**Vitality (%)**	**DFI (%)**
Control	12.0 ± 2.2	51.7 ± 3.8	64.7 ± 5.8	28.5 ± 6.6
4.9 mW	11.6 ± 2.3	51 ± 4.8	63.7 ± 5.3	27.6 ± 6.9
33 mW	11.9 ± 2.3	46.3 ± 5.3	67.0 ± 6.6	28.5 ± 7.5
p value	0.96	0.641	0.961	0.8231
H value	0.08	0.89	0.079	0.39

Legends to figures

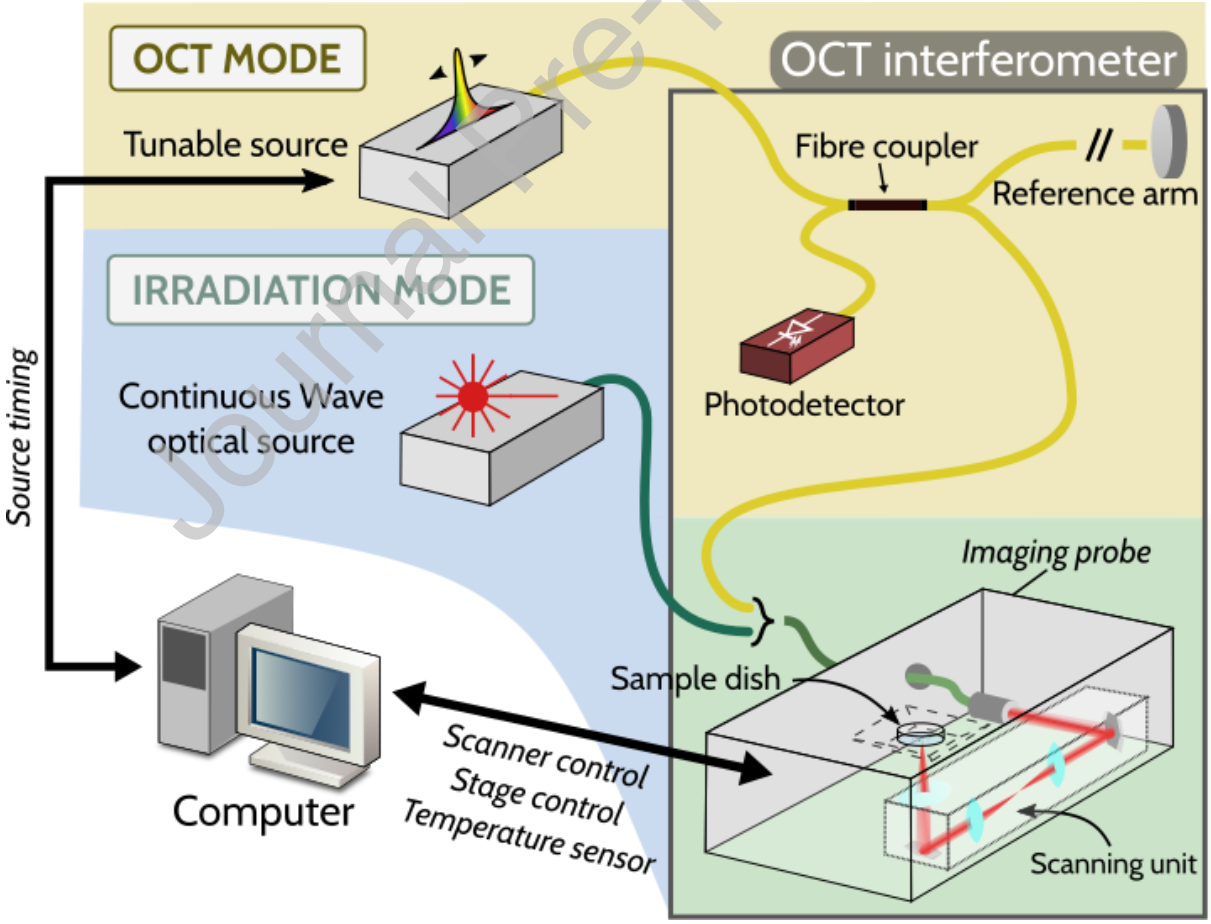

Figure 1: Schematic diagram of the optical setup for optical coherence tomography (OCT) imaging and irradiation experiments. The setup comprises two modes: Irradiation mode (represented on blue

background) and OCT mode (represented on yellow background). The OCT interferometer consists of a fibre coupler that splits light from the tuneable laser source into the sample arm and reference arm. The light in the sample arm interacts with the specimen and is collected back through the same path.

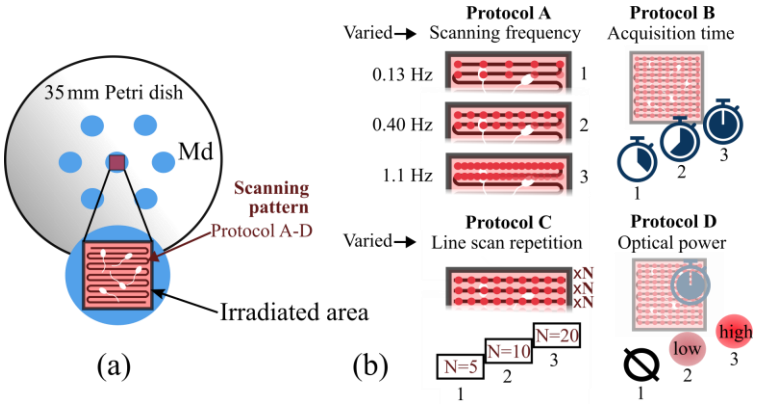

Figure 2: (a) Diagram of Petri dish and arrangement of culture media droplets. The irradiated area is shown. (b) Description of the scanning protocols (A-D) simulating the operation of a point-scanning OCT system.

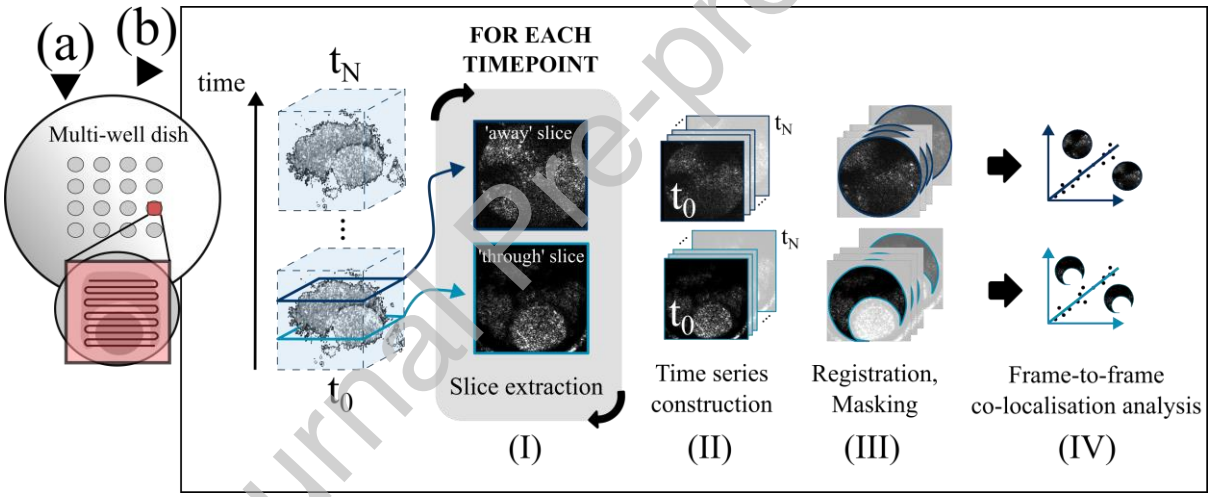

Figure 3: (a) Diagram of scanning pattern over sample in a well of a multi-well dish during the OCT timelapse of porcine COCs with irradiated sperm. (b) Image processing routine for data analysis. For each COC's 3D dataset, co-localisation analysis was performed at two depth slices, one through the oocyte surrounded by the cumulus cells and one above the oocyte, through the cumulus cells only.

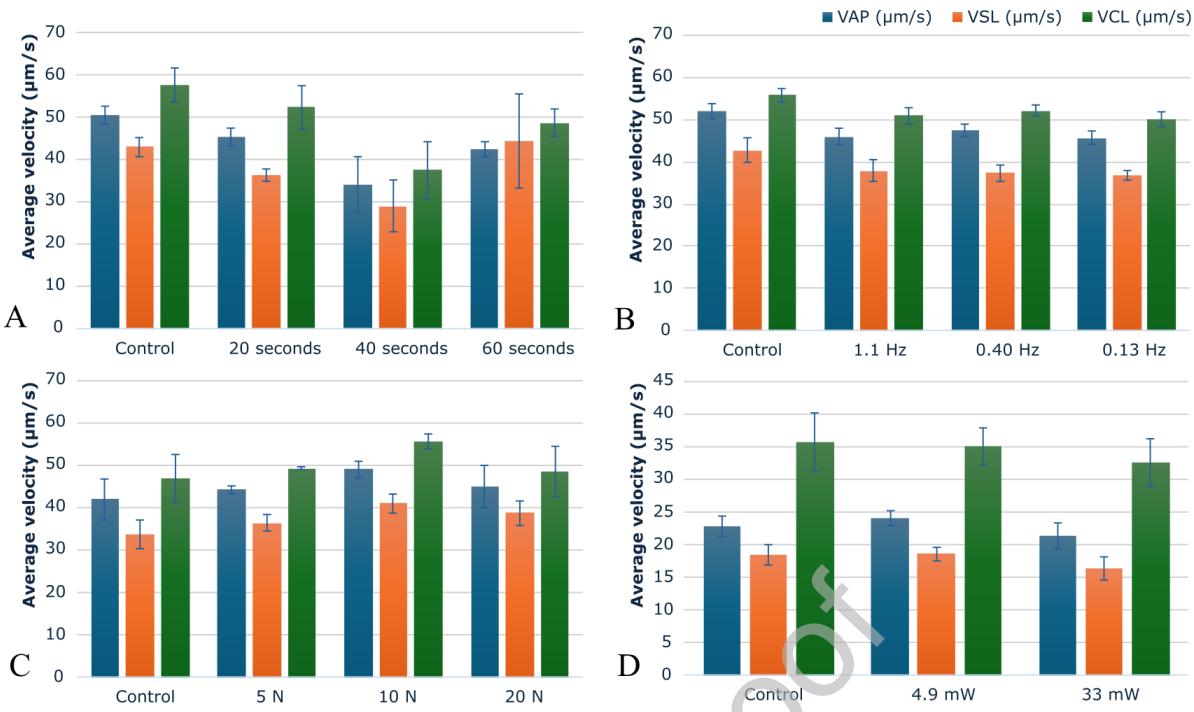

Figure 4: Boar and human sperm motility parameters when subjected to varying conditions (Protocols A-D), A: boar sperm subjected to varied overall irradiation time, B: boar sperm subjected to varied scanning frequency, C: boar sperm subjected to varying OCT-A line scan repetition and D: human sperm irradiated with two different optical powers. Control samples are non-irradiated samples. Curvilinear line velocity – VCL; straight line velocity – VSL; average path velocity – VAP. Error bars represent standard error.

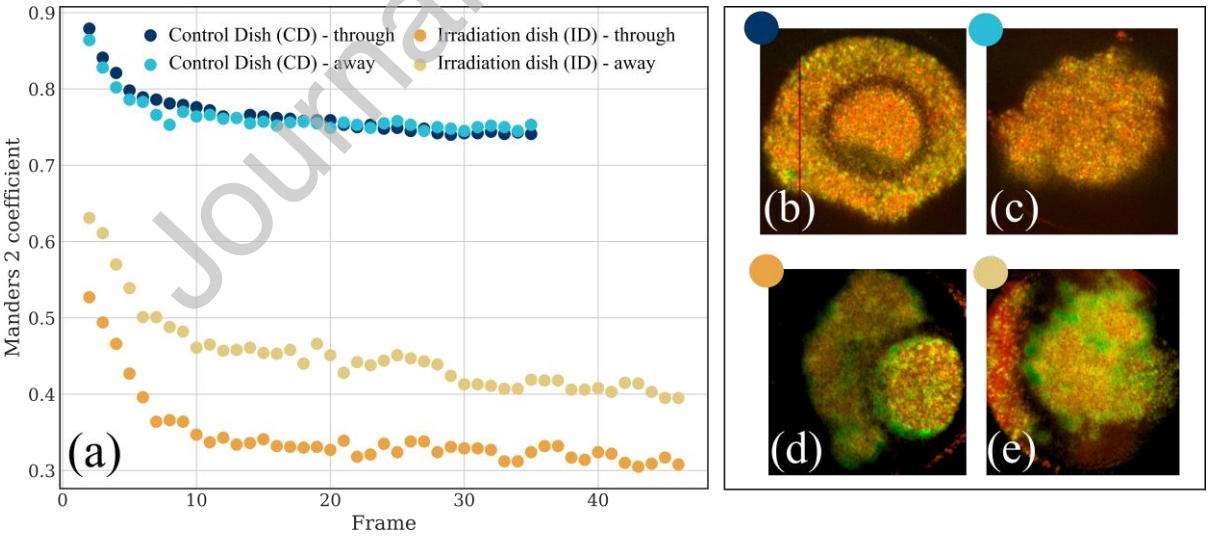

Figure 5: Analysis of sample dynamics across the timelapse duration. (a): Co-localisation analysis, evolution of M2 coefficient between a given frame and the reference frame at t_0. The evolution of M2 against time is shown in shades of blue for the control COC (CD), in shades of yellow for the irradiated COC (ID). For each sample, data from two depths is considered. (b) to (e): Logarithm Intensity Variance (LIV) maps obtained with the same frames. In LIV maps, red colour corresponds to low dynamics, green colour to high dynamics. Map brightness corresponds to the logarithmic OCT intensity.

Key Message

We investigated the genotoxic impact of broadband infrared radiation on boar and human sperm. There was no observable effect on sperm parameters following irradiation, sperm retain the ability to penetrate the cumulus, and the sperm-dependent motion of cumulus cells during co-culture can be observed in three dimensions by OCT.

Author Summary

Marie Claire Aquilina is an andrology researcher with a PhD in Biochemistry from University of Kent. Her research focuses on both animal and human andrology.